

A wind tunnel study of variability in power output of scaled wind turbine farms.

P. Martinez-Giraldo, K. M. Talluru, and K. A. Chauhan

School of Civil Engineering, The University of Sydney, NSW, 2006, Australia.

Email for correspondence: kapil.chauhan@sydney.edu.au

Abstract — This study establishes an experimental capability in the boundary layer wind tunnel at The University of Sydney to measure fluctuating power output from scaled wind turbine farms. As a first step, measurements are performed on a single scaled wind turbine, modelled as a porous disk with 58% solidity. The novelty in this study is the calibration procedure, wherein the power output of a wind turbine is directly related to the measured strain on its post. The wind turbine model is subjected to a range of wind speeds, while time-varying velocity $U(t)$, thrust force $F(t)$ and strain $\epsilon(t)$ are simultaneously measured using a Pitot-static tube (connected to a differential pressure transducer), a six-axis load balance and a strain gage assembly, respectively. Results show that the coefficient of thrust C_T for the wind turbine model varied between 0.75 and 0.85 as a function of wind speed; similar behaviour of C_T has been reported previously in the full-scale wind turbine farms [1]. Velocity measurements in the wake region of the porous disk show identical characteristics of the wake behind a rotating disk model, thus establishing that the porous disk model chosen here can be used as a surrogate to a rotating wind turbine.

Key words: Wind turbine, wind farm, power output fluctuations.

1. Introduction

One of the challenges of wind energy generation is the power output variability, which is largely due to unsteady atmospheric surface layer conditions under which wind turbines operate. It is known that the power output variability of a single wind turbine can be compensated by addition of multiple wind turbines in an array, forming what is known as a wind farm. The fluctuating power output $P(t)$ is related to the product of incoming time-varying flow velocity $U(t)$ and the thrust force $F(t)$ acting on the wind turbine, i.e., $P(t) = U(t) \times F(t)$. Substituting known relationship for drag force, it can be shown that $P(t)$ is proportional to $U^3(t)$. Thus, a challenge this study aims to address is to measure both the instantaneous velocity and drag force simultaneously for accurate estimation of power fluctuations.

2. Experimental details

Measurements are carried out in the Boundary Layer Wind Tunnel (BLWT) in the School of Civil Engineering at the University of Sydney. The BLWT is a closed-circuit wind tunnel with a working section of 19 m long, 2.5 m wide and 2 m high. The roof height is constant in the first 12 m of the test section, followed by a 5 m long blockage tolerant section, which consists of an arrangement of horizontal slats. The flow is driven by a 250 kW fan. Flow induced by the fan passes through a flow-straightener and a series of mesh screens before entering the contraction (with an area ratio of 4.5:1) and then the test section. In its current configuration, the wind

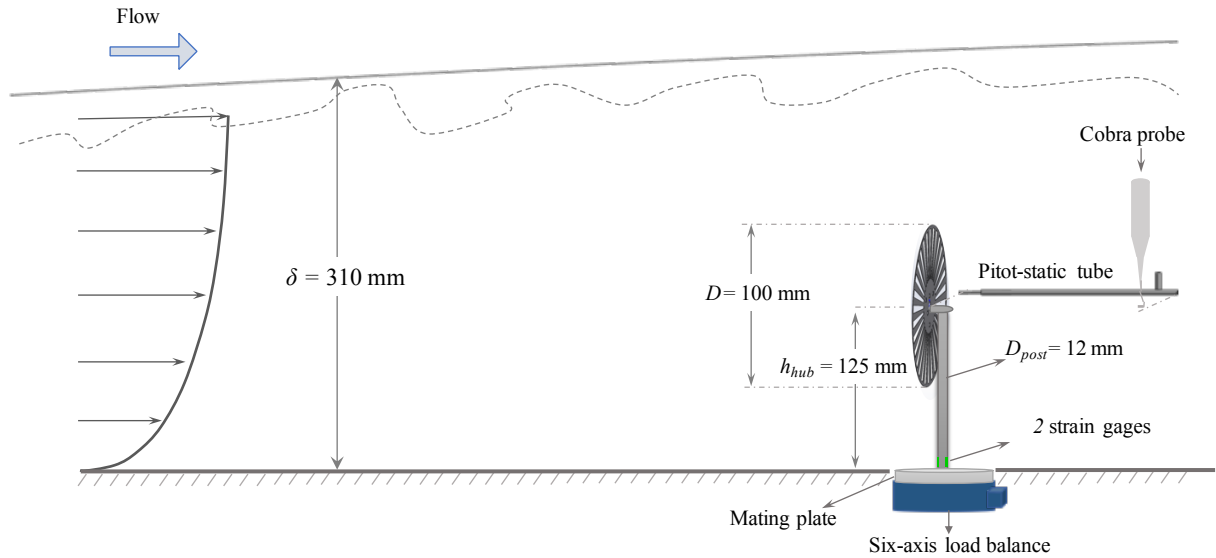


Figure 1: A schematic of the experimental setup used in this study.

tunnel is capable of generating free-stream velocity in the range of 1.4 - 27 m/s. In the current study, the flow developed on a nominally smooth surface resulting in a boundary layer thickness $\delta = 0.31$ m at the measurement location. Most of the measurements in this study are conducted at a free-stream velocity of 10 m/s, where the free-stream turbulence intensity is found to be about 0.5%.

Based on the actuator disk concept, a scaled wind turbine, modelled as a porous disk is used to approximate the full-scale wind turbine wake characteristics in the wind tunnel. Under turbulent inflow conditions, simplified porous disks for laboratory-scaled wind turbine studies have been reported to be sufficient for creating a closely similar far-wake as rotating wind turbine models [2, 3, 1]. In this study, a 30-slot-blade steel disk of 0.1 m diameter (D), 0.003 m thickness and a solidity of 58% is used to reproduce a horizontal axis wind turbine response. An acrylic rod of 0.15 m height, 0.012 m diameter and a low Young's modulus of 3.2 GPa is used as the turbine tower support, offering good strain response. To instantaneously measure the strain, a pair of FLA-5-23-3LT-type strain gages with 120Ω gage resistance and 2.16 gage factor are bonded to the bottom part of the turbine model post (cf. figure 1). The strain gages are connected in a half-bridge configuration to a National Instrument CompactDAQ data acquisition system by using a NI-9237 module with a maximum sampling rate of 50 kS/s/ch and 24-bit resolution.

The wind turbine model is attached to a highly-sensitive six-axis load cell (JR3, model 30E12A4) by using a specially designed mating plate. The force-moment sensor is held by a plate located below the tunnel floor level at the measurement location and it is used to directly measure the time-varying thrust force $F(t)$ acting on the wind turbine model. The JR3 multi-axis load cell provides analog representation of the forces along the three orthogonal axes. In addition, it also provides information about the fluctuating moments about those axes. The wind turbine model is subjected to a range of wind speeds, while $U(t)$, $F(t)$ and $\epsilon(t)$ are simultaneously measured. Thus, the power output (P) is related to the micro-strain (ϵ) through an in-situ calibration.

In order to establish the porous disk model as an equivalent representation of a rotating disk model for wind tunnel studies, we have conducted two sets of measurements - (i) to quantify the wake behind the turbine and (ii) to document the coefficient of thrust force as well the

relationship between power output and the strain on the wind turbine post. These are discussed in detail in the following sections.

3. Wake measurements

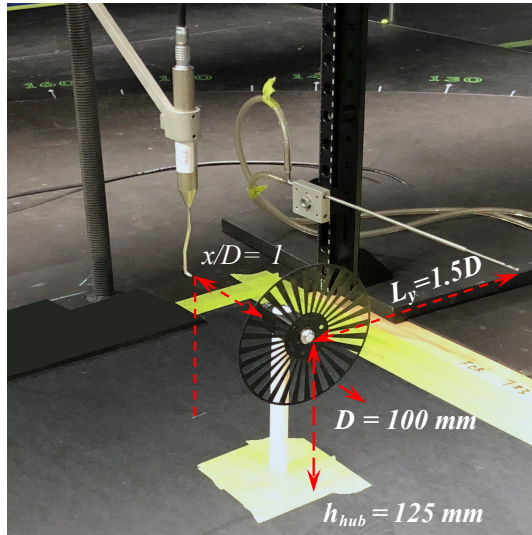


Figure 2: Experimental setup used for measuring the wake profile behind the porous disk.

0 mm $\leq y \leq 200$ mm, fixing the disk centroid as the horizontal reference ($y = 0$). Same number of points are measured in vertical direction between 25 mm $\leq z \leq 200$ mm (z is distance from the ground), with reference hub height, h_{hub} equal to 0.125 m. At each measurement point, data are acquired for 180 seconds with a sampling frequency of 8192 Hz after passing through a digital low-pass filter at 4096 Hz.

Figures 3 (a & b) show the comparison of mean streamwise velocity defect and turbulence intensity, respectively against the results for stationary and rotating wind turbine models from the literature [1, 4]. Note that figure 3(a) is normalised by the maximum velocity defect and the half-wake thickness, $y_{1/2}$. Results from the current study are in very good agreement with those for rotating and non-rotating turbine models. It appears that the velocity defect profiles at $x/D = 3$ and 5 closely resemble the Gaussian profile that is expected in the far-wake region. On the other hand, there are clear discrepancies in the turbulence intensity profiles for different turbine models at $x/D = 3$ (refer to figure 3b), which are primarily due to differences in the incoming flow conditions and the thrust coefficients of turbine models. Nonetheless, the profiles of turbulence intensity are qualitatively similar. Although the measurements are limited to a maximum distance of $x/D = 5$, it is expected that the agreement between stationary and rotating wind turbine models will improve further downstream.

4. Force and strain measurements

In practice, the fluctuations in the power output of a wind turbine occur at a wide range of time scales or frequencies, which is due to turbulence in the incoming flow, weather conditions and wind-structure interactions in the upstream wind turbines. Hence, a second most important requirement for a scaled wind turbine model is the measurement of thrust force with high fre-

In order to measure the wake characteristics, the porous disk model is tested in the scaled wind-turbine assembly (as shown in figure 2) so that the influence of developing boundary layer on the wake structure is truly quantified. Wake measurements are performed using a Cobra-probe (TFI, Australia) and a single-axis traversing system. The Cobra probe is a four-hole pressure probe, which resolves all the three velocity components and local static pressure over a range of wind speeds (2-100 m/s), with a frequency response up to 2000 Hz. The single-axis traversing system has a resolution of 1-micron and is mounted in different orientations to carry out velocity measurements in the transverse and vertical directions. Measurements are taken at three downstream locations ($x/D = 1, 3$ & 5), as well as at $x/D = -1$ to characterise the incoming velocity profile. For the present study, 21 linearly spaced measurement points are taken in the spanwise direction between

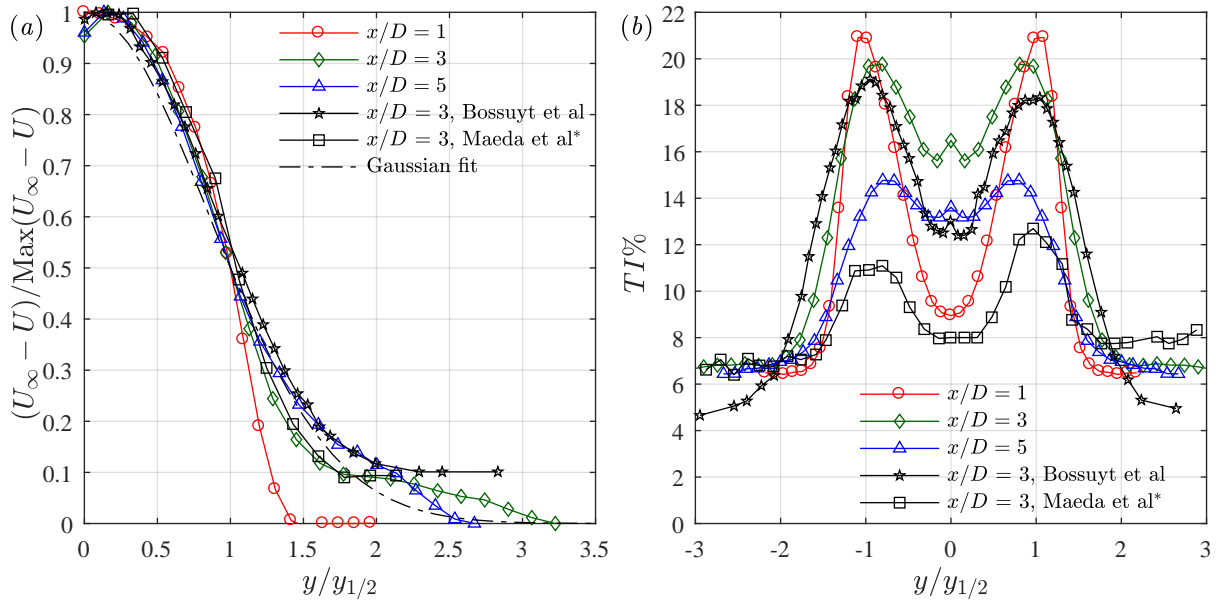


Figure 3: Wake measurements of normalised (a) streamwise velocity defect and (b) turbulence intensity at three downstream distances, $x/D = 1, 3$ and 5 , compared against previous experimental results of rotating and non-rotating turbine models [1, 4].

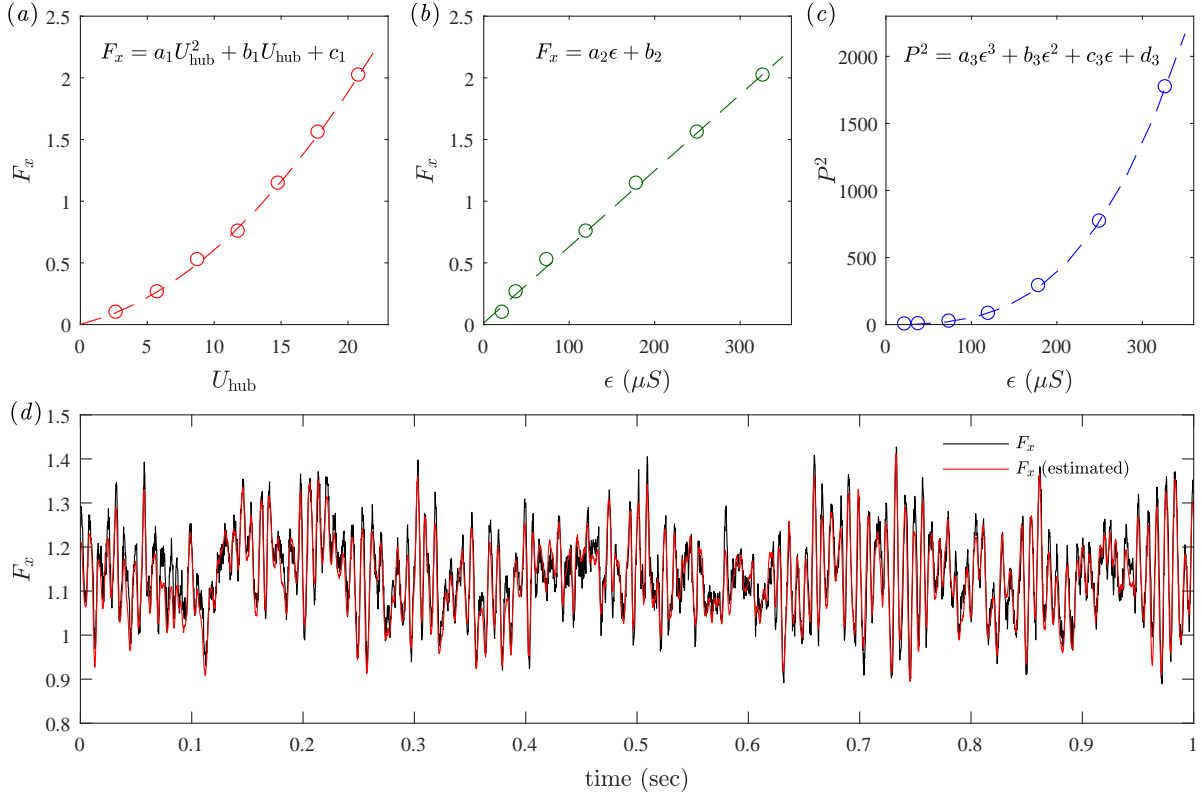


Figure 4: Experimentally obtained functional relationship between (a) F_x and U_{hub} ; (b) F_x and ϵ ; (c) P^2 and ϵ . (d) Comparison of measured and estimated forces.

quency response. Further, it is crucial to truly capture the large-scale or low-frequency eddies in the flow as they are most energetic. To this end, a second set of experiments are conducted to characterise the dynamic behaviour of the porous disk model used in this study. The time-varying force, strain and velocity are simultaneously measured using a six-axis load cell, strain gage assembly and a Pitot-static tube connected to a fast-responsive pressure transducer with an accuracy of $\pm 0.1\%$. In our initial tests, it is found that the characteristic frequency of the porous disk assembly is approximately 60 Hz and hence all the instrumentation (with frequency response greater than 300 Hz) used in this study are able to sufficiently measure all the energetic eddies corresponding up to 150 Hz. For improving the sensitivity of the strain-gages as well as to eliminate any temperature effects on strain, a set of two strain-gages are arranged in a half-bridge configuration, giving a strain output twice that obtained from a single strain-gage. Further, the strain-gages are mounted very close to the mounting point, where the strain is expected to be the maximum for a beam fixed at one end. Finally, the Pitot-static tube is positioned at the hub height as one would expect the velocity at that location to be the important reference velocity.

Measurements are performed over a range of wind speeds between 3 m/s and 23 m/s for a period of 180 seconds to quantify the variation of thrust force, strain, power output as a function of wind speed. Figure 4(a) shows the time-averaged force F_x plotted as a function of U_{hub} . It is clearly evident that F_x increases with U_{hub} in a quadratic relationship. The thrust coefficient, C_T , is then calculated using F_x as,

$$C_T = \frac{F_x}{1/2\rho U_{\text{hub}}^2 A_D}, \quad (1)$$

where ρ is the density of air and A_D is the swept area of the disk. It is observed that the thrust coefficient varied between 0.75 and 0.85 as a function of wind speed. These results are consistent with previous wind tunnel studies of non-rotating turbine models, e.g., [1] and is within the range of thrust coefficient values reported for the commercial full-scale wind turbines [5, 6].

4.1. Validation of calibration procedure

One of the key contributions of the current study is the dynamic calibration of the strain gages, which is later used to estimate thrust force and power output of the turbine model. The calibration relationship between F_x and ϵ is shown in figure 4(b), which clearly indicates linear behaviour between the thrust force and the strain measured on the model post. To establish the accuracy of this procedure, we have compared the force (directly measured using six-axis load cell) and the force (F_x – estimated) estimated by applying calibration on the strain-gage data. These results are presented in figure 4(d), which shows excellent agreement between the measured and estimated forces establishing the accuracy of the calibration procedure.

4.2. Estimating power output from strain

With the availability of measurements of $F(t)$, $U(t)$ and ϵ , it is possible to establish a link between time-averaged power output P and strain. At first, power is computed using the relationship, $P(t) = U(t) \cdot F(t)$, which implies that $P(t) \propto U^3(t)$ as it was shown in figure 4(a) that $F(t) \propto U^2(t)$. Further, it is seen that $F(t) \propto \epsilon$, which implies that P^2 and ϵ are related via a third-order polynomial. Indeed, the results presented in figure 4(c) clearly establish this. Now, one can use the functional relationship between P^2 and ϵ to estimate the time-varying power output using the fluctuating signal from the strain-gage assembly as done in figure 5.

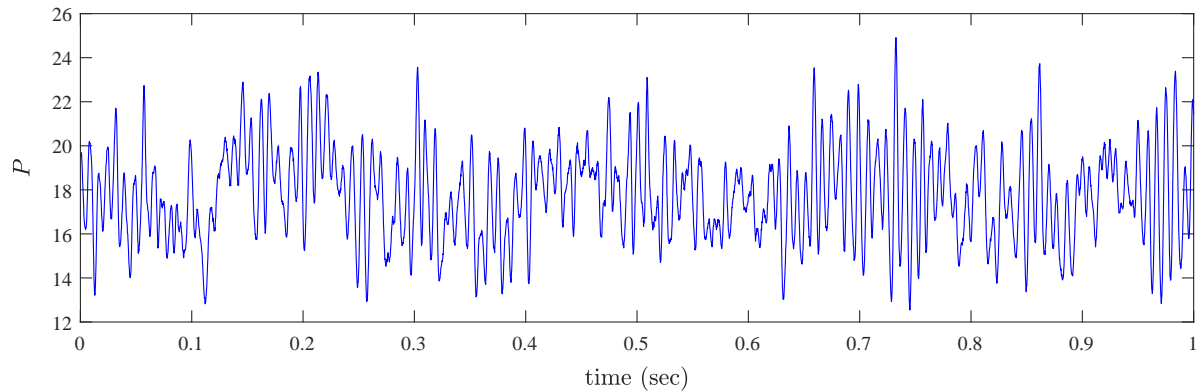


Figure 5: Power estimated using the fluctuating strain signal.

5. Conclusions

An experimental facility has been developed and tested to study the power output fluctuations of a single wind turbine model. A novel calibration procedure has been implemented, wherein, the force acting on the wind turbine is related to the strain measured on its post. Results show excellent agreement between measured and estimated forces. The procedure is further developed to estimate the power output variations based on the strain measurements on the wind turbine post. In conclusion, the results clearly establish the experimental method developed for studying the power output fluctuations of a single wind turbine. As a future goal of this study, this experimental procedure will be further expanded to study the power output variations of a wind turbine farm consisting of an array of porous disk models similar to the one studied here.

References

1. J Bossuyt, M F Howland, C Meneveau, and J Meyers. Measurement of unsteady loading and power output variability in a micro wind farm model in a wind tunnel. *Exp. Fluids*, 58(1):1, 2017.
2. L P Chamorro and F Porté-Agel. Effects of thermal stability and incoming boundary-layer flow characteristics on wind-turbine wakes: a wind-tunnel study. *Bound-layer Meteorol.*, 136(3):515–533, 2010.
3. S Aubrun, S Loyer, P E Hancock, and P Hayden. Wind turbine wake properties: Comparison between a non-rotating simplified wind turbine model and a rotating model. *J. Wind Eng. Ind. Aerodyn.*, 120:1–8, 2013.
4. T Maeda, Y Kamada, J Murata, S Yonekura, T Ito, A Okawa, and T Kogaki. Wind tunnel study on wind and turbulence intensity profiles in wind turbine wake. *J. Thermal Sci.*, 20(2):127–132, 2011.
5. F Porté-Agel, Y Wu, and C Chen. A numerical study of the effects of wind direction on turbine wakes and power losses in a large wind farm. *Energies*, 6:5297–5313, 2013.
6. C. Desmon, J. Murphy, L. Blonk, and H. Wouter. Description of an 8 mw reference wind turbine. *J. Phys.: Conf. series*, 753, 2016.